Communication

Portable Magnetic Field Mapping Measurement System based on Large-Scale Dipole Magnets in HIAF

Xiang Zhang *, Zi Di Wu, Li an Jin, Jing Yang, Xian Jin Ou, Dong Sheng Ni, Yue Cheng, Li Xia Zhao, Tong Jin Tong, Wei Gang Dong, Bei Min Wu, Guo Hong Li, Qing Gao Yao *

Posted Date: 20 December 2024

doi: 10.20944/preprints202412.1764.v1

Keywords: magnetic field measurement; large-scale dipole magnet; ultrasonic motors

 doi:10.20944/preprints202412.1764.v1

Communication

Portable Magnetic Field Mapping Measurement System based on Large-Scale Dipole Magnets in HIAF

Xiang Zhang [1,2,*], Zidi Wu [1], Li'an Jin [1,2], Jing Yang [1,2], Xianjin Ou [1,2], Dongsheng Ni [1,2], Yue Cheng [1], Lixia Zhao [1], Yujin Tong [1], Weigang Dong [1], Beimin Wu [1] and Guohong Li [1] and Qinggao Yao [1,2,*]

[1] Institute of Modern Physics, Chinese Academy of Sciences, No. 509 Nanchang Rd., Lanzhou 730000, Gansu Province, P. R. China
[2] School of Nuclear Science and Technology, University of Chinese Academy of Sciences, No. 19 Yuquan Rd., Beijing 100049, P.R. China
* Correspondence: zhangxiang@impcas.ac.cn (X.Z.); yaoqinggao@impcas.ac.cn (Q.G.Y.); Tel.: +86 18509316716 (X.Z.); Tel.: +86 18509316711 (Q.G.Y.)

Abstract: The High-Intensity Heavy-Ion Accelerator Facility (HIAF) is a significant national science and technology infrastructure project, constructed by IMP, to provide primary and radioactive intense beams for nuclear and related research. Large aperture, high-precision, and warm-ion superconducting dipole magnets are extensively utilised to achieve high beam intensities. However, the traditional Hall point measurement platform faces limitations such as magnet volume, measurement environment, and the range of good field regions in the measurement of large dipole magnets, especially huge superconducting dipole magnets, leading to poor operability, low measurement efficiency, and significant errors in secondary positioning accuracy. This paper introduces a new magnetic field mapping measurement system, which introduces ultrasonic motors capable of operating under strong magnetic fields (<7T), and can realize portable, efficient and high-precision magnetic field measurement. After system debugging, the SRing dipole magnet prototype was measured. The system's accuracy and efficiency were verified through comparison with traditional Hall probe measurement systems. On this basis, magnetic field distribution and integral excitation curve measurements of all 11 HFRS warm-iron superconducting dipole magnets and 3 HFRS anti-irradiation dipole magnets were carried out and completed, achieving the testing objectives.

Keywords: magnetic field measurement; large-scale dipole magnet; ultrasonic motors

1. Introduction

The High-Intensity Heavy-Ion Accelerator Facility (HIAF), as shown in Figure 1 [1], is a significant national science and technology infrastructure project constructed by the Institute of Modern Physics, Chinese Academy of Sciences. Which is scheduled to be completed in 2025, and will provide a low-energy heavy ion beam with extremely high peak current intensity [2-4]. To achieve high beam intensities, large room-temperature and warm-iron superconducting dipole magnets are extensively utilised in HIAF, including the Booster Ring (BRing) dipole magnets, high-precision Spectrometer Ring (SRing) dipole magnets, and HIAF Fragment Separator (HFRS) dipole magnets [4-7]. The project required magnetic field distribution and excitation curve measurements for each Synchrotron reference dipole magnet and all HFRS dipole magnets. Due to the huge size and complex cryogenic system, the magnet is difficult to move during the test, especially superconducting magnets.

 doi:10.20944/preprints202412.1764.v1

In magnetic field measurement of accelerator magnets, the traditional Hall probe measurement technology relies on a massive three-dimensional measurement platform, coupled with a three-dimensional adjustable magnet support frame, offering great universality and high positional accuracy in measuring medium and small magnets. Such as the CMM bench with three orthogonal axes at ANL, the mapping device in GSI, the CERN PS magnet mapping bench, the IMP mapping device, and the ESRF Hall probe Bench [8-10]. This faces limitations such as magnet volume, measurement environment, and the range of good field regions in measuring large dipole magnets, especially huge superconducting dipole magnets. This leads to poor operability, low measurement efficiency, and significant errors in secondary positioning accuracy. Based on the traditional Hall point measurement platform, the BRing dipole magnet prototype is tested by a long coil combined with the Gauss meter based on the Hall probe [11]. This system can measure the I-BL curve efficiently, but cannot realise field distribution measurement, and the length of the device is about equal to double the lengths of the magnets and occupies a large space. In recent years, the GSI team designed a system based on induction-coil sensors translated in the dipole magnet's bore to measure the Super-FRS dipole magnets [12]. This system has the advantage of quickly measuring the integral magnetic field uniformity but is not suitable for magnetic field distribution measurement. In the HESR dipole magnet measurement, GSI designed a new device for measuring the high-order field components of the magnetic field using the ultrasonic motor, making it possible to apply the transmission mechanism in the magnet air gap [13].

To achieve the magnetic field distribution test goal of the HIAF large dipole magnet, an efficient and high-precision movable magnetic field distribution test system is necessary. Based on the ultrasonic motor which can operate under strong magnetic fields (<7T), a new portable magnetic field mapping system, which can be placed in the magnet air gap, is designed. This greatly reduces the size of the test system, shortens the measurement time and improves the test efficiency. After the system debugging, the accuracy and efficiency of the new test system are verified by comparing it with the traditional point test system. On this basis, the tests of 11 superconducting dipole magnets and 3 rectangular anti-irradiation dipole magnets at HFRS are completed.

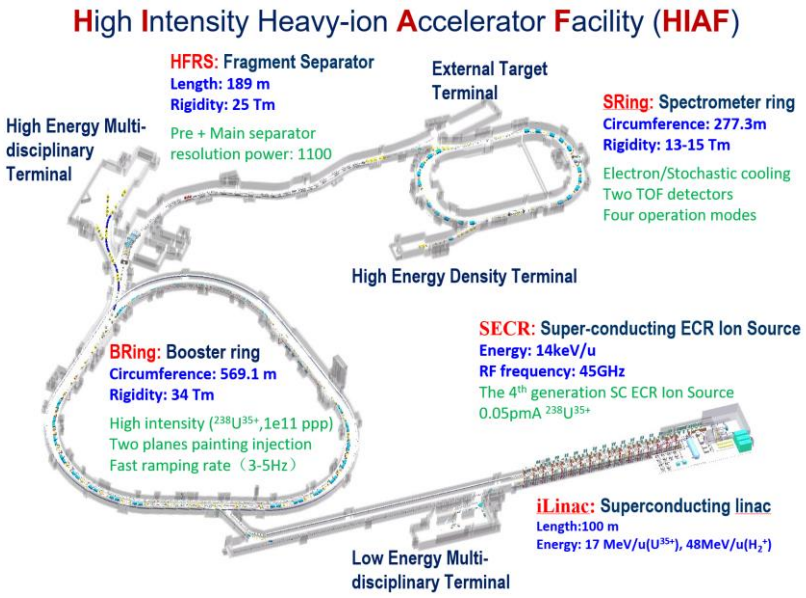

Figure 1. The layout of HIAF.

 doi:10.20944/preprints202412.1764.v1

2. Materials and Methods

This chapter will introduce the portable magnetic field mapping measurement system in detail, including general design, system composition, measurement method and coordinate calculation.

2.1. The General Design

The design of the system mainly has 3 aspects:

(1) The ultrasonic motor using, which can work under strong magnetic fields, makes it possible to place the platform inside the magnet gap and drive the arm to rotate under a strong magnetic field, radically reducing the size and weight of the test system.

(2) The gaps of dipole magnets are limited. The rotating motion inside the magnet instead of the traditional horizontal linear motion, further reduces the mechanical size of the test system. At the same time, the length of the rotating arm is reduced, so that it can be quickly stabilized after stopping, which greatly reduces the stability time of the measuring rod and improves the test efficiency.

(3) The maximum angular resolution of the ultrasonic motor is limited to 360°/2500. Using the 1:4 dual-gear, the angular resolution is increased to 360°/10000, and the position resolution is improved to 0.09mm.

2.2. The Components of the Portable Magnetic Field Mapping Measurement System

The composition of the measuring system is shown in Figure 2:

(1) The rail with a translational stroke of 4300mm when testing the HFRS warm-ion superconducting magnets, and lengthened to 5300mm when testing the HFRS anti-irradiation magnets.

(2) The slider platform on which the ultrasonic motor, the encoder, and the replaceable rotating arm are placed.

(3) The ultrasonic motor and the encoder have stable operation under a strong magnetic field (< 7T).

(4) The rotating arm, has an initial length of 280mm, for mounting the Hall sensor, and the length can be changed.

(5) The axial motion servo motor and conveyor belt, are used to transfer the sliding platform to the magnet air gap.

(6) The motion control and data acquisition system, are used to realize motion control, magnetic field and current acquisition.

(7) Group 3's DTM151 Gauss meter and MPT141 Hall probe.

(8) Nuclear magnetic resonance instrument (NMR), used to check the magnetic field of the Gauss meter before the formal test, to ensure the accuracy of the Gauss meter itself and the fixed.

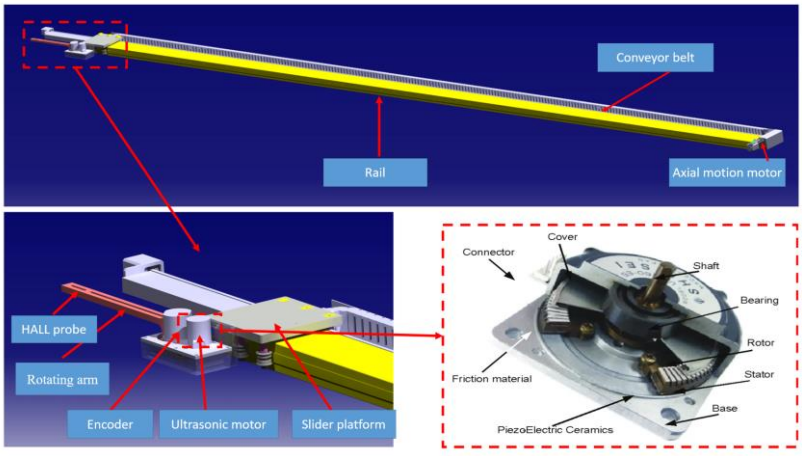

Figure 2. The components of the measurement system.

2.3. The Magnetic Field Measurement Method and Coordinate Calculation

The magnetic field measurement uses the traditional point-to-point method: The slider platform and rotating arm are driven to move the Hall sensor to the measured point, then trigger the Gauss meter and data acquisition instrument by the encoder to collect the magnetic field and current. Test the next point until the magnetic field measurement of all points is completed.

In the Cartesian coordinate system, the path of a dipole magnet is a series of parallel arcs with a deflection radius. However, the position coordinates of the measurement system are composed of a

Preprints.org (www.preprints.org) | NOT PEER-REVIEWED | Posted: 20 December 2024 doi:10.20944/preprints202412.1764.v1

linear motion variable (L_i) in the Cartesian coordinate system and a rotational angle variable (θ_i) in the local coordinate system moving with the slider platform. Therefore, the arc path coordinates need to be geometrically transformed to the new coordinate system for testing.

The Cartesian coordinate system is established with the motor end of the rail as the origin; the local coordinate system is established with the ultrasonic motor as the origin, and the Angle between the rotating arm and the rail is (θ_i). As shown in Figure 3.

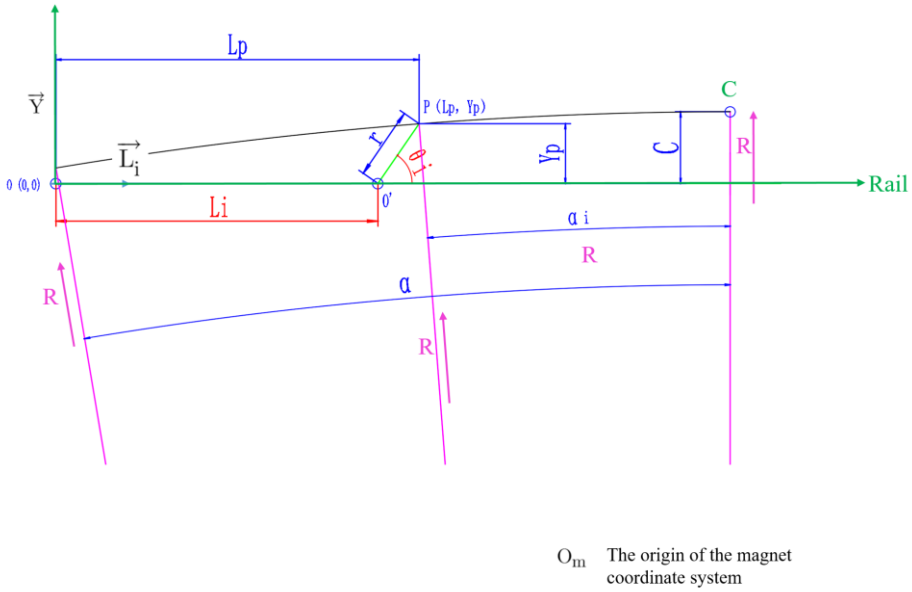

Figure 3. The parallel arcs and the coordinate conversion diagram.

The description of the parameters in Figure 3 is shown in Table 1.

Table 1. The parameters of Figure 3.

Parameters	description
R	The radius of the dipole magnet
r	The radius of the rotating arm
L_i	linear motion variable
θ_i	rotational angle variable
α_i	$\angle CO_M P$
α	$\angle CO_M O$

The coordinate transformation of the linear motion variable (L_i) and rotational angle variable (θ_i) as shown:

In Cartesian coordinates, the coordinates of any point in an arc are expressed as follows:

$$L_p = R \times \left(\sin(\alpha) - \sin(\alpha_i)\right) = L_i + r \times \cos(\theta_i) \tag{1}$$

$$Y_p = C - R \times \left(1 - \cos(\alpha_i)\right) = r \times \sin\theta_i \tag{2}$$

Solve the equations, the linear motion variable (L_i) and a rotational angle variable (θ_i) as shown:

$$\theta_i = \arcsin\left(\frac{C - R \times \left(1 - \cos(\alpha_i)\right)}{r}\right) \tag{3}$$

$$L_i = R \times \left(\sin(\alpha) - \sin(\alpha_i)\right) - r \times \cos(\theta_i) \tag{4}$$

The specific coordinates can be solved by Python.

 doi:10.20944/preprints202412.1764.v1

3. Results

3.1. The Magnet Parameters and Measurement Requirements for SRing and HFRS Dipole Magnets

The parameters and requirements are shown in Table 2 and Table 3.

Table 2. The magnets parameters.

Parameters	SRing dipole magnets	HFRS warm-ion superconducting dipole magnets	HFRS anti-irradiation dipole magnets	unit
Number	20	11	3	/
Range of magnetic field	0.21-1.66	0.22-1.6	0.21-1.6	T
Reference magnetic field	1.1	0.83	0.83	T
Gap	±52	±70	±103	mm
Good field region (H×V)	318×80 (0.84-1.39T) 236×80 (0.21-1.66T)	±160×±62	±160×±90	mm
Bending radius	9.5	15.7	15.7	m
Deflection angle	18	10	10	°
Edge angle	0	0	0	°
Integral field homogeneity	$\pm3\times10^{-4}$ (318×80@1.10T) $\pm5\times10^{-4}$ (220×80@1.66T) $\pm3\times10^{-4}$ (240×80@0.21T)	$\pm3\times10^{-4}$ (0.2~1.2T)	$\pm3\times10^{-4}$ (0.83T) $\pm8\times10^{-4}$ (1.60T)	/
Maximum current	1780	210	1600	A
weight	45000	52000	81000	kg

Table 3. The magnetic field measurement requirement.

Items	SRing dipole magnets	HFRS warm-ion superconducting dipole magnets	HFRS anti-irradiation dipole magnets
Number	1	11	3
I-BL curve	Imax=1780 A	Imax=210 A	Imax=1600
Magnetic field distribution	0.21T, 1.1T, 1.66T	0.22T, 0.83T, 1.6T	0.21T, 0.83T, 1.6T

3.2. The Measurement of SRing Dipole Magnets

3.2.1. System Debugging

After the system is built, we use a laser tracker to test and debug the accuracy of the system's motion position. The position accuracy test is divided into two parts: the linear motion along the rail and the rotating motion along the ultrasonic motor's rotating shaft.

When measuring the position accuracy of linear motion along the guide rail, 30mm is used as the test step, and the total test length is 4320mm (longer than the test range of the SRing dipole magnet). The test results are shown in Figure 4. The maximum deviation of a single-step size movement is less than 0.1mm, the average distance of actual movement is 29.999mm, and the average deviation is -0.0005mm. The deviation value is considered to meet our test requirements.

When measuring the rotational accuracy, the Angle step is 2° and the total measurement Angle is 90°. The results show that the maximum deviation of a single step size is 0.048°, the average rotation Angle is 2.0008° and the average deviation is 0.0008°. The deviation value is also considered to meet the test requirements.

 doi:10.20944/preprints202412.1764.v1

3.2.2. The Comparison between the Traditional Hall Probe Magnetic Field Mapping Measuring System and the Portable Magnetic Field Mapping Measuring System to Measure SRing Dipole Magnet

After system debugging, the magnetic field of the SRing dipole magnet was measured to verify the accuracy and efficiency of the system.

Figure 4a. shows the SRing dipole magnet measurement photo using the traditional Hall mapping measurement system, and Figure 4b. shows the measurement photo using the portable magnetic field mapping measurement system.

Figure 5. shows the integral field homogeneity of the SRing dipole magnet. It can be seen that the difference between the two systems is less than 1×10^{-4}. The stability and the measurement accuracy of the new system are verified well.

It is worth emphasising that the time step of the traditional magnetic field measurement system is about 20 seconds per point, and the new system takes only about 1.6 seconds per point. The test efficiency improves more than 10 times.

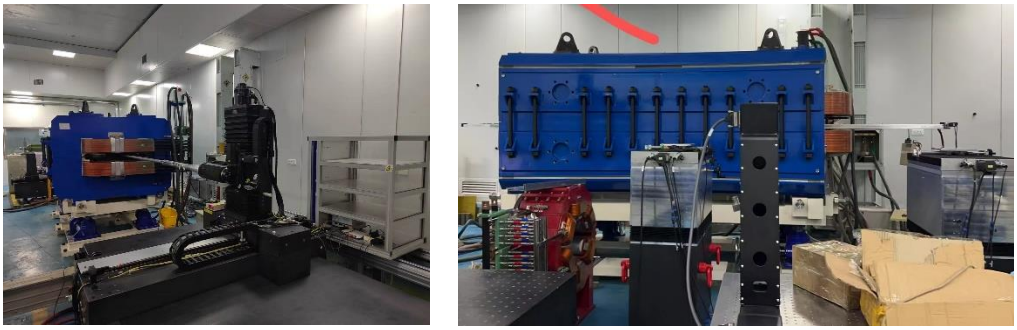

(**a**) (**b**)

Figure 4. (a) SRing dipole magnet test by the traditional Hall mapping measurement system; **(b)** SRing dipole magnet test by the portable magnetic field mapping measurement system.

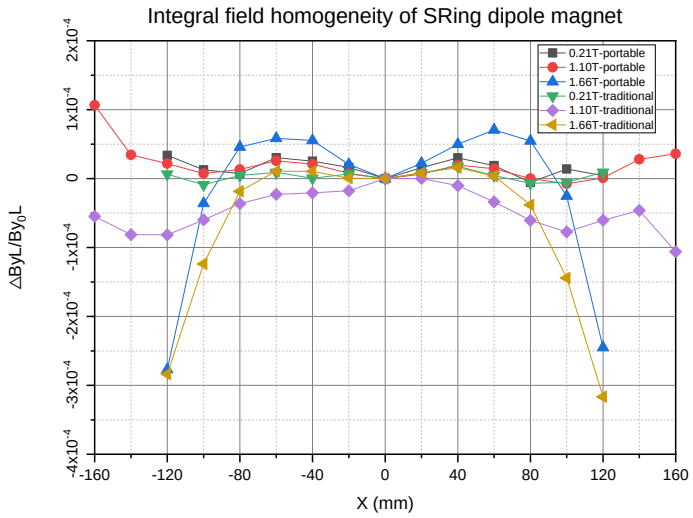

Figure 5. The comparison of the integrated field homogeneity of SRing dipole magnet.

 doi:10.20944/preprints202412.1764.v1

3.3. The Magnetic Field Batch Measurement of the HFRS Warm-Iron Superconducting Dipole Magnets and the HFRS Anti-Irradiation Dipole Magnets

Based on the measurement and verification of the magnetic field of the SRing dipole magnet, the magnetic field distribution and integral excitation curve measurements of 11 HFRS warm-iron superconducting dipole magnets and 3 anti-irradiation dipole magnets were carried out and completed. The measurement results of the two kinds of magnet prototypes are as follows:

Figure 6a. shows the photo of HFRS superconducting dipole magnet measurement, and Figure 6b. shows the photo of HFRS anti-irradiation dipole magnet measurement.

Figure 7a. shows the integral field homogeneity of the HFRS warm-iron superconducting dipole magnet, and Figure 7b. shows the integral field homogeneity of the HFRS anti-irradiation dipole magnet.

Figure 8a. shows the I-BL curve of the HFRS warm-iron superconducting dipole magnet, and Figure 8b. shows the I-BL curve of the HFRS anti-irradiation dipole magnet.

So far, all 11 warm-iron superconducting dipole magnets of HFRS have been tested, and the test results meet the design requirements.

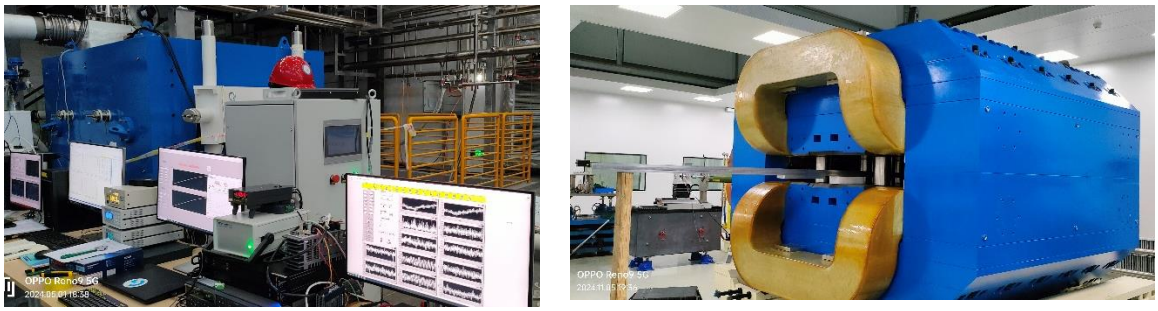

(**a**) (**b**)

Figure 6. (a) Test of HFRS warm-iron superconducting dipole magnet; **(b)** Test of HFRS anti-irradiation dipole magnet.

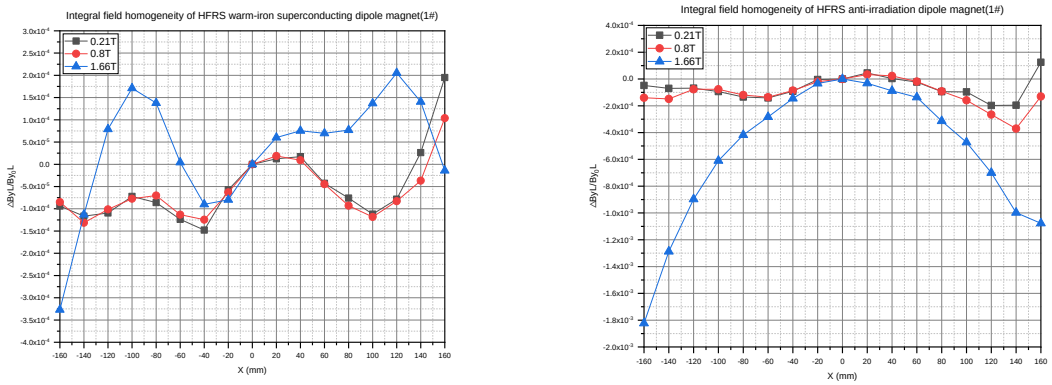

(a) (b)

Figure 7. (a) The integral field homogeneity of HFRS superconducting magnet (1#); **(b)** The integral field homogeneity of HFRS anti-irradiation dipole magnet (1#).

 doi:10.20944/preprints202412.1764.v1

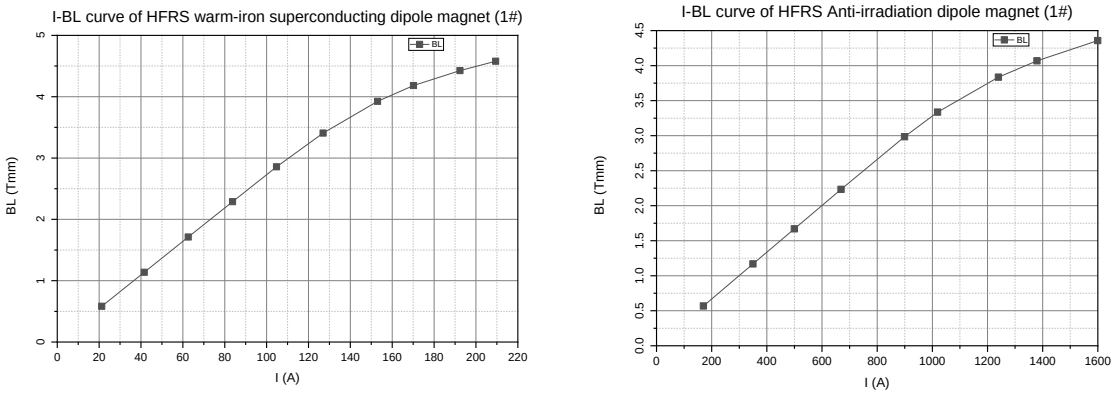

(a) (b)

Figure 8. (a) The I-BL curve of HFRS superconducting magnet (1#); **(b)** The I-BL curve of HFRS anti-irradiation dipole magnet (1#).

4. Discussion

In order to measure the magnetic field distribution of large dipole magnets, especially of large superconducting dipole magnets, a portable magnetic field mapping measurement system is designed. On this basis, the magnet test target of HIAF project was completed. This provides a method for other similar magnet tests. In the future, we will further develop a curved orbit measurement device for magnet measurement with different deflection radius.

5. Conclusions

The design and application of the portable magnetic field mapping measuring system based on the ultrasonic motor can effectively improve the magnetic field measurement efficiency of large-scale (superconducting) magnets. The time step takes only about 1.6 seconds per point, the testing accuracy was verified through comparison and analysis with traditional Hall probe measurement systems. So far, all 11 warm-iron superconducting dipole magnets and 3 Anti-irradiation dipole magnets of HFRS have been tested, and the test results meet the requirements.

Author Contributions: Conceptualization, Xiang Zhang and Qinggao Yao; methodology, Xiang Zhang and Zidi Wu; software, Li'an Jin, Zidi Wu, and Jing Yang; validation, Xiang Zhang and Qinggao Yao; formal analysis, Xiang Zhang, Zidi Wu, Li'an Jin, and Lixia Zhao; investigation, Zidi Wu, Li'an Jin, Xianjin Ou, and Yujin Tong; resources, Dongsheng Ni, Yue Cheng, and Weigang Dong, Beimin Wu; data curation, Zidi Wu, Li'an Jin, Lixia Zhao, and Xiang Zhang; writing—original draft preparation, Xiang Zhang; writing—review and editing, Xiang Zhang and Qinggao Yao; visualisation, Xiang Zhang; supervision, Qinggao Yao; project administration, Xiang Zhang and Qinggao Yao; funding acquisition, Qinggao Yao, and Guohong Li. All authors have read and agreed to the published version of the manuscript.

Funding: This research was funded by the Lanzhou Science and Technology project, grant number E139973SQ0; and the High Intensity heavy-ion Accelerator Facility (HIAF) approved by the National Development and Reform Commission of China, grant number 2017-000052-73-01-002107. The APC was funded by the Lanzhou Science and Technology project, grant number E139973SQ0.

Data Availability Statement: No new data were created.

Acknowledgements: The authors wish to thank the technical team of Hefei Micro Precision Control Instrument Technology Co., LTD for their help in the process of developing the test system.

Conflicts of Interest: The authors declare no conflicts of interest. The funders participate in the project management.

 doi:10.20944/preprints202412.1764.v1

References

1. X. Zhang, L.M. Ma, Optimization design and test of the Booster Ring dipole magnet in HIAF. Jinst, 2022, 17(03), P03024.
2. J.C. Yang*, J.W. Xia. High Intensity heavy ion Accelerator Facility (HIAF) in China. NIMB, 2013, 317, 263-265.
3. Ma X, Wen W Q. HIAF: New opportunities for atomic physics with highly charged heavy ions. NIMB, 2017, 408, 169-173.
4. Xiaohong Zhou*, Jiancheng Yang. Status of the high-intensity heavy-ion accelerator facility in China. AAPPS Bull., 2022, 32, 35.
5. B. Wu, J.C. Yang. The design of the Spectrometer Ring at the HIAF. NIMA, 2017, 881, 27-35
6. Sheng L N, Zhang X H. Ion-optical design of High energy Fragment Separator (HFRS) at HIAF. NIMB, 2020, 469, 1-9.
7. Beimin Wu, Wei You. Mechanical Design, Construction and Testing of the Superferric Dipoles for the High Energy Fragment Separator of the HIAF. IEEE, 2024, 34, 5
8. G. Moritz. MECHANICAL EQUIPMENT. CERN ACCELERATOR SCHOOL, Europa Palapa Hotel, Anacapri, Italy, 11-17 April 1997, 251-257.
9. He Yuan. Magnetic Measurement System for CSR and Its Applications. Doctor of Philosophy, University of Chinese Academy of Sciences, Beijing, June 2003.
10. Lucas Samaille, Gaël Le Bec, Reine Versteegen. Update of the magnetic measurement benches of the ESRF. The 23rd International Magnetic Measurement Workshop, Bad Zurzach, Switzerland, 6-11 October 2024.
11. ZHANG Xiang, JIN Li'an. Magnetic Field Measurement System of the BRing Fast Ramping Dipole Magnet in HIAF. NPR, 2022, 39(4), 470-475
12. G. Golluccio, M. Buzio. Instruments and methods for the magnetic measurement of the super-FRS magnets. Proceedings of IPAC2016, Busan, Korea. May 8-13 2016.
13. Jan Henry Hetzel, J¨urgen B¨oker. Development of a Field Mapper for the Determination of the Multipole Components of the Curved HESR Dipole Magnets. IEEE, 2018, 28 (3), 1-4.